Supporting Information

A General Approach towards Carbonization of Plastic Wastes into Well-designed 3D Porous Carbon Framework for Super Lithium-Ion Batteries

Jiakang Min,[a,f] Xin Wen, [b] Tao Tang,[a*] Xuecheng Chen,[b*] Kaifu Huo,[c*] Jiang Gong,[d] Jalal Azadmanjiri,[e] Chaobin He[f] and Ewa Mijowska[b]

[a.] State Key Laboratory of Polymer Physics and Chemistry, Changchun Institute of Applied Chemistry, Chinese Academy of Sciences; Changchun 130022, China.

[b.] Faculty of Chemical Technology and Engineering, West Pomeranian University of Technology, Szczecin, Piastów Ave. 42, 71-065 Szczecin, Poland.

[c.] Wuhan National Laboratory for Optoelectronics (WNLO) and School of Optical and Electronic Information, Key Laboratory for Material Chemistry of Energy Conversion and Storage, Ministry of Education, School of Chemistry and Chemical Engineering, Huazhong University of Science and Technology, Wuhan 430074, China.

[d.] Key Laboratory of Material Chemistry for Energy Conversion and Storage, Ministry of Education, Hubei Key Laboratory of Material Chemistry and Service Failure, School of Chemistry and Chemical Engineering, Huazhong University of Science and Technology, Wuhan 430074, China.

[e.] Faculty of Science, Engineering and Technology, Swinburne University of Technology, Hawthorn, Victoria, 3122 Australia.

[f.] Department of Materials Science & Engineering, National University of Singapore, 9 Engineering Drive 1, Singapore 117576, Singapore.

Corresponding author: ttang@ciac.ac.cn; xchen@ciac.ac.cn; kfhuo@hust.edu.cn

Experimental section

Materials: The plastic wastes (PP, PE, PS, PVC, and the corresponding mixtures) were obtained from real-world commercial polymer packaging. Magnesium oxide (MgO), hydrochloric acid (HCl, 5%), and ethanol (98%) were purchased from China National Medicines Corporation Ltd, and ferric acetylacetonate ($Fe(acac)_3$) was brought from Sigma-Aldrich. The chemicals were used as received without purification.

Synthesis of MgO/Fe(acac)$_3$ template: The universal binary combined template is constructed by mixing flake structured porous MgO and $Fe(acac)_3$ in ethanol to obtain a solid template $MgO/Fe(acac)_3$, the mass ratio of MgO to $Fe(acac)_3$ is 1:1.

Synthesis of HCS/PCF: In a typical synthesis, 2 g of $MgO/Fe(acac)_3$ and 0.2 g of polymer waste were mixed and introduced into a stainless autoclave at room temperature. The autoclave was sealed and heated at 700 ^oC for 2 h. After cooling down to room temperature, the black solid samples were collected and rinsed with dilute HCl to remove the template. In the next step, the 3D hierarchical HCS/PCF nanomaterials (HCS/PCF) were filtered and rinsed with deionized water for several times and subsequently dried in vacuum at 80 ^oC for 8 h. For comparison, the $MgO/Fe(acac)_3$ template was also carbonized alone in steel autoclave to get MgO/Fe_3O_4 product. The Fe_3O_4 residues are 10.7, 11.2, 10.3, 11.9, 6.5 wt% for PP, PE, PS, PVC, and their mixture derived HCS/PCF, respectively. According to the different carbon resource utilized, the corresponding carbon products are named as: PS: HCS/PCF, PP: HCS/PCF, PVC: HCS/PCF, PE: HCS/PCF, Mixture: HCS/PCF.

Characterization

The morphology and microstructure of the samples were examined by field-emission scanning electron microscopy (FE-SEM, JEOLJEM-1011) at 100 kV, transmission electron microscopy (TEM, FEI G2 S-T), and high-resolution transmission electron microscopy (HR-TEM, FEI G2 S-Twin transmission electron microscope operated at 200 kV). The relative molecular weight of PS foam was determined by gel permeation chromatography (GPC) on TOSOH HLC 8220 GPC at 40 ℃ using THF as an eluent against linear polystyrene standards. The phases were determined by X-ray diffraction (XRD, D8 advance X-ray diffractometer) with Cu Kα radiation at 40 kV and 200 mA. The thermal stability of the samples was evaluated by thermal gravimetric analysis (TGA) under flowing air at a heating rate of 10 K/min on the TA Instrument SDT Q600. The vibrational properties were characterized by

Raman scattering (T6400, excitation-beam wavelength: 514.5 nm) and the porosity was measured by nitrogen adsorption/desorption at 77 K on a Quantachrome Autosorb-1C-MS analyzer. The elemental analysis was performed by X-ray photoelectron spectroscopy (XPS) on the VG ESCALAB MK II spectrometer using Al Kα radiation from an X-ray source (10.0 kV and 10 mA).

Electrochemical Measurement

The electrochemical experiments were carried out using 2032 coin-type cells. The working electrodes were prepared by mixing HCS/PCF, carbon black (C-NERGY SUPER C65, Timcal), and polyvinylidene difluoride (PVDF, Solef 5130, Solvay) with a weight ratio of 80:10:10 and pasting onto Cu foils (Schlenk Metallfolien GmbH & Co.). A lithium foil (Aldrich) was used as the counter electrode and the electrolyte consisted of a solution of 1 M $LiPF_6$ in ethylene carbonate (EC)/dimethyl carbonate (DMC) (1:1 by volume). The cells were assembled in an argon-filled glove box with less than 1 ppm moisture and oxygen. The electrochemical properties were determined in the voltage range between 0.01 and 3.0 V by the galvanostatic charging/discharging technique.

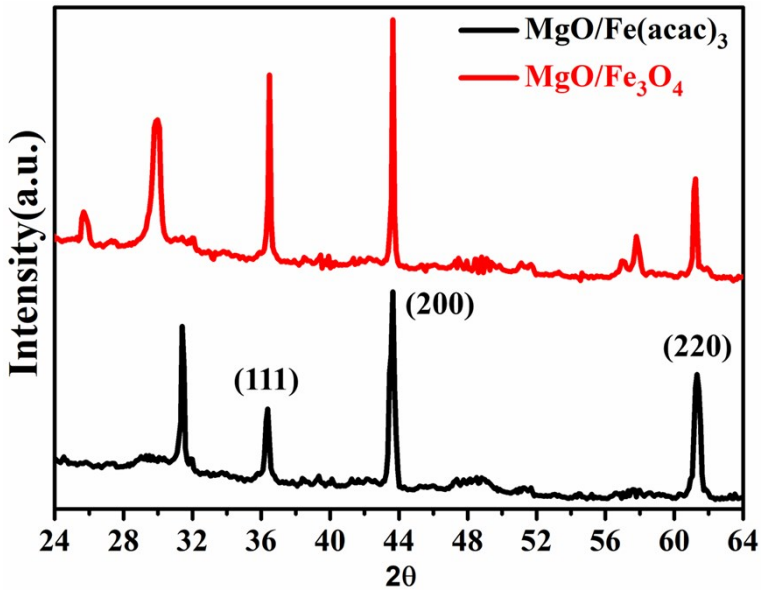

Figure S1. XRD patterns of $MgO/Fe(acac)_3$ and carbonization product in N_2 ($C/MgO/Fe_3O_4$).

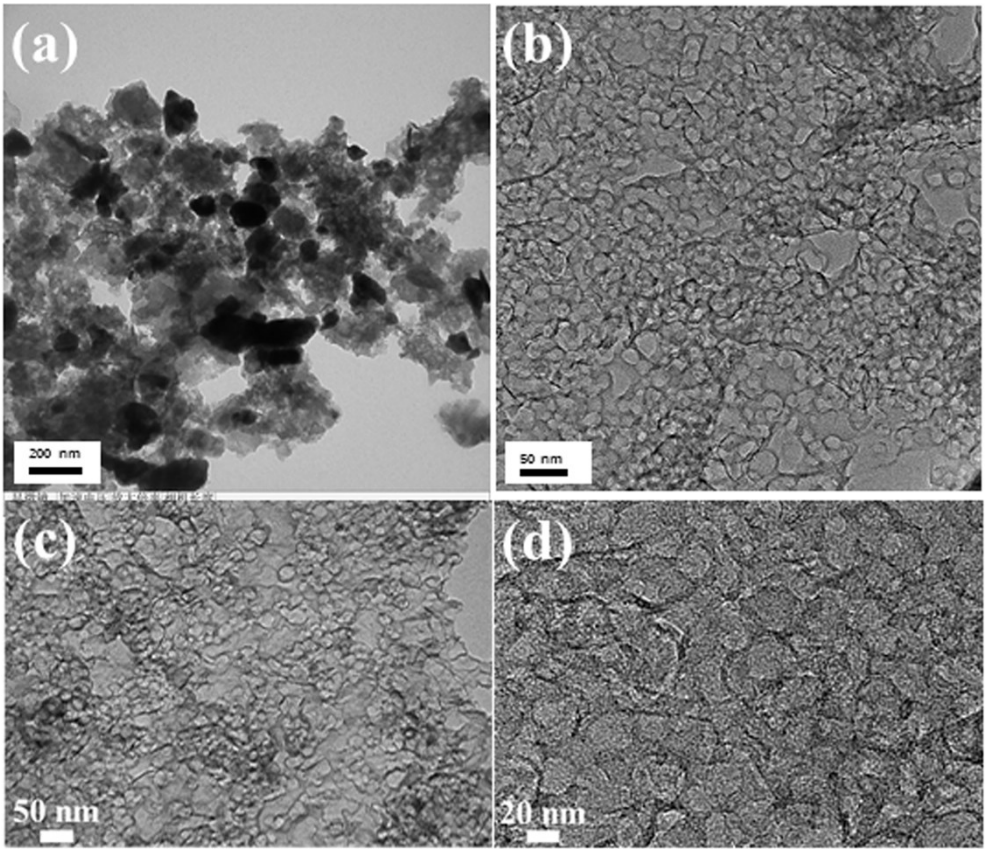

Figure S2. TEM image of (a) $Fe(acac)_3/MgO/PS$ carbonization product before HCl treatment. (b) HCS/PCF derived from PE and a mixture of PS, PE, PP, and PVC (c, d).

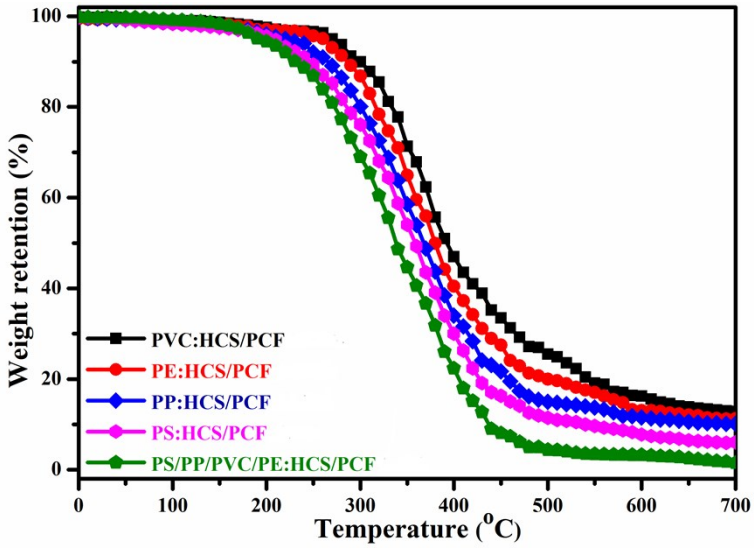

Figure S3. TGA curves of HCS/PCF samples from different polymers.

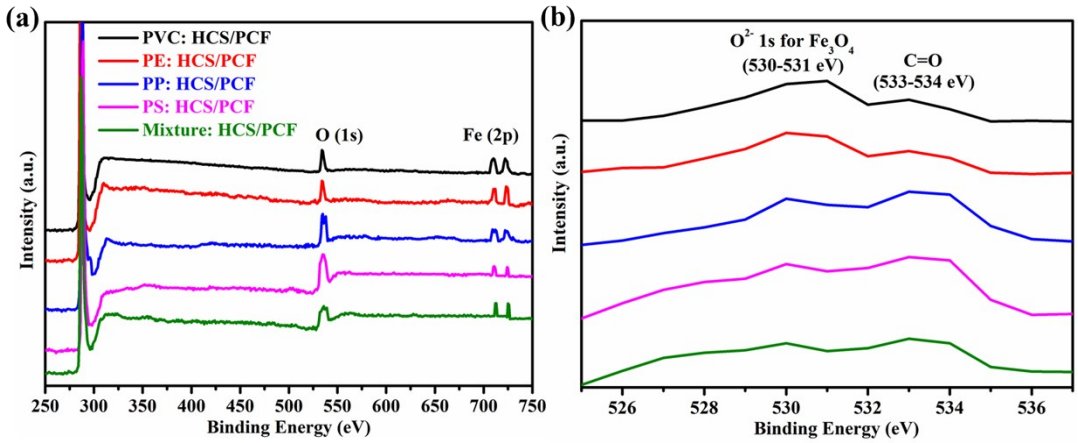

Figure S4. (a) XPS spectra of HCS/PCF samples. (b) High resolution XPS spectra of oxygen peaks of HCS/PCF.

High-resolution O1s XPS spectrum is further deconvolved into two single peaks at 530.3 and 533.5 eV, which are associated with the O^{2-}1s for Fe_3O_4 and C=O group, respectively. Notably, O^{2-}1s species is the majority of PVC: HCS/PCF and PE: HCS/PCF, while C=O group is predominant for PP: HCS/PCF, PS: HCS/PCF and mixture: HCS/PCF, which is related to the oxygen-carbon bonding configurations transition in different carbon sources.

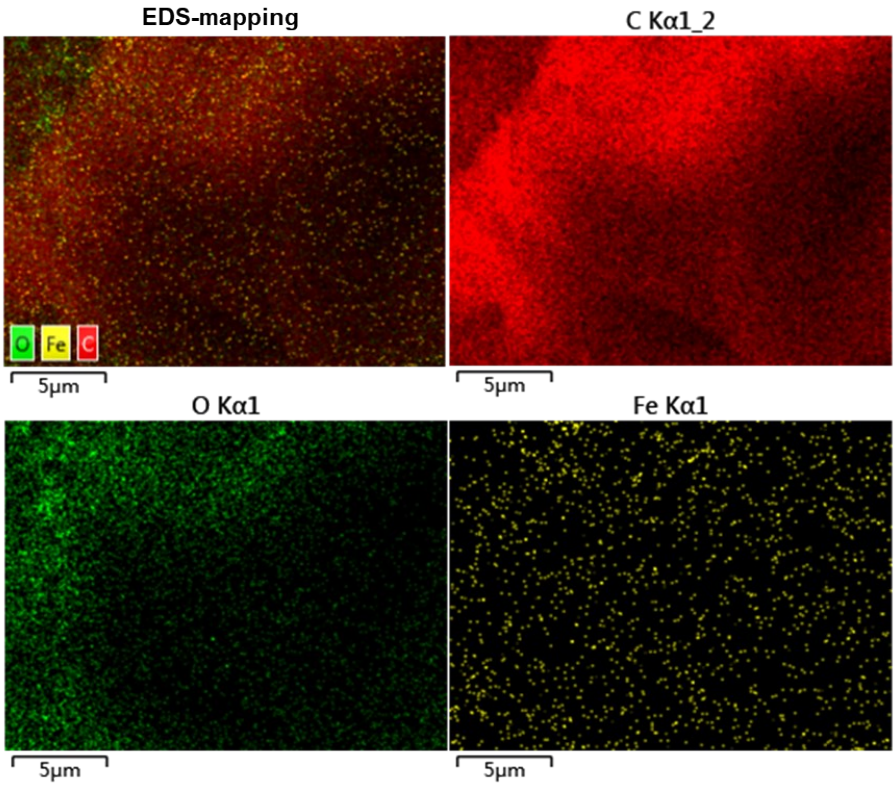

Figure S5. SEM-energy-dispersive spectra elemental mapping of HCS/PCF.

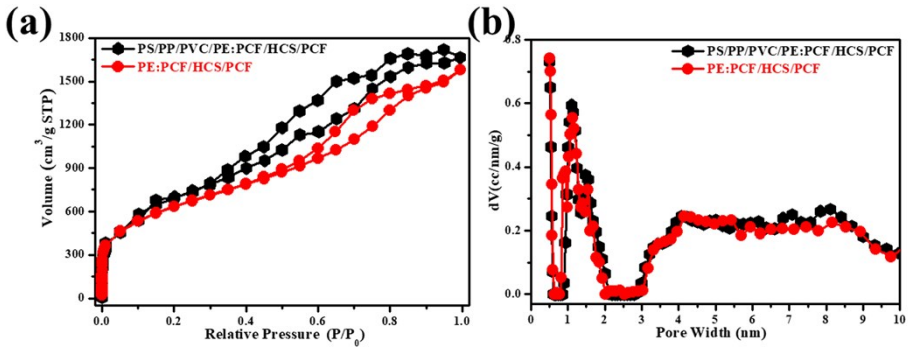

Figure S6. N_2 sorption/desorption isotherms and pore size distribution of HCS/PCF from PE and polymer mixtures.

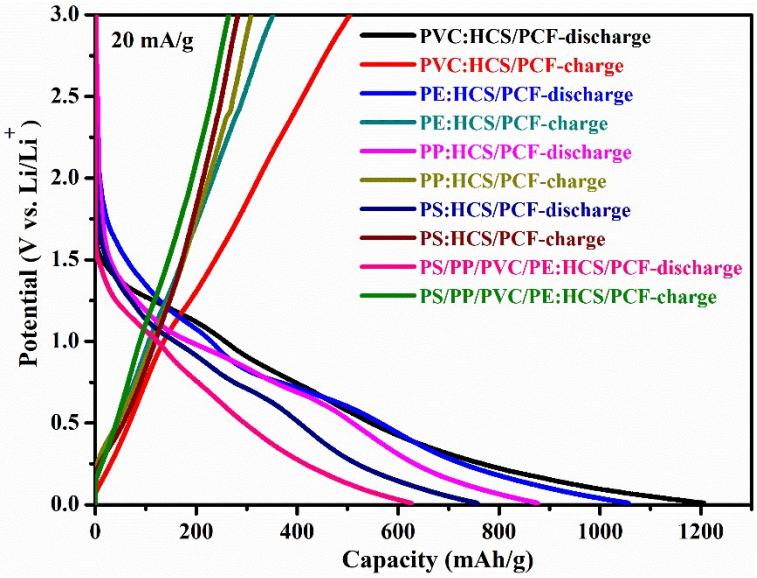

Figure S7. First charge/discharge profiles of HCS/PCF from different polymers.

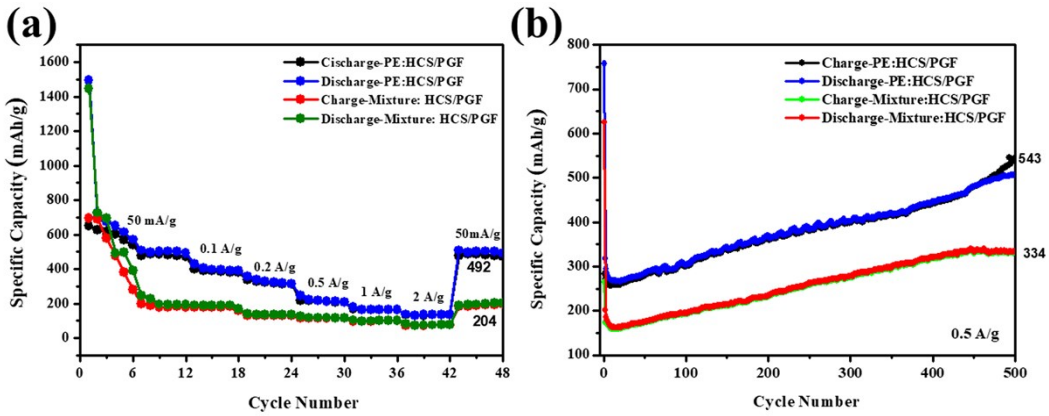

Figure S8. (a) Rate performance and (b) long cycle stability of HCS/PCF derived from PE and polymer mixtures.

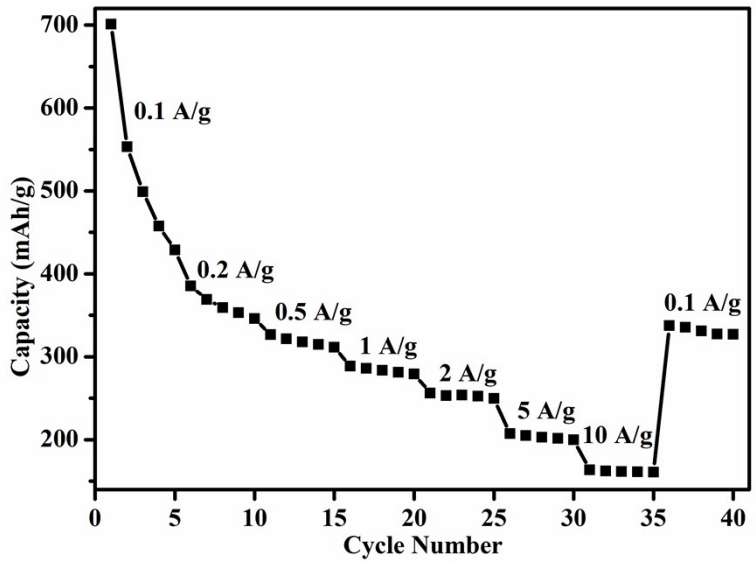

Figure S9. Rate performance of porous carbon flakes derived from the MgO template when PS was used as a carbon source.

Table S1. Textural properties of HCS/PCF samples from different polymers.

Samples	S_{BET} (m^2/g)	V_{total} (cm^3/g)
PVC: HCS/PCF	1245	4.45
PE: HCS/PCF	1282	4.48
PP: HCS/PCF	1296	4.49
PS: HCS/PCF	1344	4.52
PS/PP/PVC/PE: HCS/PCF	1382	4.68

Table S2. Comparison of the reported results in the literature.

Materials	Fe_3O_4 loading	Capacity	Cycles	Current density	References
GNS/Fe_3O_4	86.7%	580 mAh/g	100	0.7 A/g	Chem. Mater. 2010, 22, 5306
Fe_3O_4-GNS	62%	650 mAh/g	100	0.1 A/g	Chem. Eur. J. 2011, 17, 661-667
Fe_3O_4@GS/GF	83.7%	1059 mAh/g	150	0.093 A/g	Adv. Mater. 2013, 25, 2909
N-G/Fe_3O_4	30%	1130 mAh/g	200	0.1 A/g	J. Mater. Chem. A 2013, 1, 14658
GF@Fe_3O_4	80%	785 mAh/g	500	1 C	Nano Lett. 2013, 13, 6136
Fe_3O_4@C	45.4%	610 mAh/g	100	0.05 A/g	Nano Energy 2014, 8, 126

Fe_3O_4/C	99.57%	800 mAh/g	235	0.1 A/g	J. Mater. Chem. A 2014, 2, 16008
IONP@mC	39.4%	560 mAh/g	500	2 A/g	Adv. Funt. Mater. 2014, 24, 319
Fe_3O_4 NCs-GAs	67%	577 mAh/g	300	5.2 A/g	Chem. Commun. 2015, 51, 1597
G-Fe_3O_4-GNRs	60%	708 mAh/g	300	0.4 A/g	Adv. Energy Mater. 2015, 5, 1500171
MWCNTs-Fe_3O_4-rGO	53%	680 mAh/g	100	0.2 A/g	Nano Res. 2015, 8, 1339
G@Fe_3O_4@C	69%	1200 mAh/g	100	0.2 A/g	J. Mater. Chem. A 2015, 3, 7036
G/Fe_3O_4@C	69.2%	743 mAh/g	400	1.86 A/g	J. Mater. Chem. A 2015, 3, 2361
Fe_3O_4-NS/G	74.3%	445 mAh/g	600	2 A/g	Carbon 2015, 86, 310
Fe_3O_4/C@GA	22%	634 mAh/g	1000	6 A/g	Chem. Eur. J. 2016, 22, 4454
HCS/PCF-Fe_3O_4	10.7%	802 mAh/g	500	0.5 A/g	Present work